IAC-12-C4.4.6

High-Power Hall Propulsion Development at NASA Glenn Research Center

Hani Kamhawi*
NASA Glenn Research Center, USA, hani.kamhawi-1@nasa.gov

David H. Manzella[t], Timothy D. Smith[:t], and George R. Schmidt[§]

The NASA Office of the Chief Technologist Game Changing Division is sponsoring the development and testing of enabling technologies to achieve efficient and reliable human space exploration. High-power solar electric propulsion has been proposed by NASA's Human Exploration Framework Team as an option to achieve these ambitious missions to near Earth objects. NASA Glenn Research Center is leading the development of mission concepts for a solar electric propulsion Technical Demonstration Mission. The mission concepts are highlighted in this paper but are detailed in a companion paper. There are also multiple projects that are developing technologies to support a demonstration mission and are also extensible to NASA's goals of human space exploration. Specifically, the In-Space Propulsion technology development project at the NASA Glenn has a number of tasks related to high-power Hall thrusters including performance evaluation of existing Hall thrusters; performing detailed internal discharge chamber, near-field, and far-field plasma measurements; performing detailed physics-based modeling with the NASA Jet Propulsion Laboratory's Hall2De code; performing thermal and structural modeling; and developing high-power efficient discharge modules for power processing. This paper summarizes the various technology development tasks and progress made to date.

ACRONYMS

BN	boron nitride
$D_{T,m}$	mean thruster diameter, meter
EDU	engineering development unit
EP	electric propulsion
ESMD	Exploration Systems Development Directorate
ESR&T	Exploration System Research and Technology
ETDD	Engineering Technology Development and Demonstration
GaN	gallium nitride
GCD	Game Changing Division
HARP	high-speed axially reciprocating probe
HEFT	Human Exploration Framework Team
HiVHAc	High Voltage Hall Accelerator
HEOMD	Human Exploration and Operations Mission Directorate
$I_{B,250}$	intensity of boron at a wavelength of 250 µm
I_d	discharge current, A
IEPC	International Electric Propulsion Conference
ISP	In-Space Propulsion
I_{sp}	specific impulse, sec
ISTP	In-Space Transportation Program
JIMO	Jupiter Icy Moons Orbiter
JPL	Jet Propulsion Laboratory
MFAM	magnetic-field-aligned computational mesh
MOSFET	metal oxide semiconductor field effect transistors
NASA	National Aeronautic and Space Administration
NEO	near Earth objects
OES	optical emission spectroscopy
OCT	Office of the Chief Technologist
PMAD	power management and distribution
PPU	power processing unit
RPA	retarding potential analyzer
SAA	space act agreement
SCCM	standard cubic centimeter per minute
SEP	solar electric propulsion
SiC	silicon carbide
TDM	Technical Demonstration Mission
V_d	discharge voltage, V
VF5	vacuum facility 5
VF8	vacuum facility 8
η_A	anode efficiency

I. INTRODUCTION

High-power electric propulsion (EP) systems are enabling and enhancing for time-critical missions or missions requiring transportation of large payloads. A number of mission studies were performed over the last decade which highlight the enhancing and

* NASA GLENN, USA, hani.kamhawi-1@nasa.gov.
t NASA GLENN, USA, david.manzella@nasa.gov.
:t NASA GLENN, USA timothy.smith@nasa.gov.
§ NASA GLENN, USA, george.schmidt@nasa.gov.

enabling features of high-power EP systems for reusable space tug applications for transfer of payloads from low-Earth-orbit to geosynchronous-Earth-orbit and for use in Mars mission scenarios.[1,2,3]

National interest in high-power EP systems has been renewed. In 2010, NASA's Human Exploration Framework Team (HEFT) concluded that the use of a high-power (i.e., on the order of 300 kW) solar electric propulsion (SEP) system could significantly reduce the number of heavy lift launch vehicles required for a human mission to a near Earth asteroid.[4] Hall thrusters are ideal for such applications because of their high-power processing capabilities and their efficient operation at moderate specific impulses (~2000 sec), which leads to reduced trip times for such missions.[5]

NASA's Human Exploration and Operations Mission Directorate (HEOMD) Enabling Technology Development and Demonstration (ETDD) Program was focused on developing, maturing, testing, and demonstrating the technologies needed to reduce the cost and expand the capability of future space exploration activities. The ETDD Program content included performing foundational research and studying of the requirements and potential designs of advanced, high-energy in-space propulsion systems. These high-energy propulsion systems were intended to support deep space human exploration and reduce travel time between Earth's orbit and future destinations for human activity. This would enable a new space transportation capability via a SEP stage. The SEP stage could enable cost-effective missions within Earth orbit, near Earth objects (NEOs), and deep space robotic science missions. In 2011, the ETDD Program transitioned to NASA's Office of the Chief Technologist (OCT) but the program content remained and is still focused on developing, maturing, and demonstrating the high-power propulsion technologies needed to enhance the Agency's capabilities to explore and move large payloads in space. To that extent, there are several projects in the OCT Game Changing Division (GCD) that support technology development which will result in the SEP Technical Demonstration Mission (TDM) flight development. One of the key projects under OCT GCD is the In-Space Propulsion (ISP) project. This paper provides a brief overview of the SEP TDM project, additional details of the SEP TDM project are provided in a companion paper.[6] This paper provides a detailed summary of the OCT ISP technology tasks and activities over the past 2 years.

II. SOLAR ELECTRIC PROPULSION TECHNICAL DEMONSTRATION MISSION

The SEP TDM project is currently a pre-Phase A formulation activity focused on developing high value mission concepts for a demonstration mission that address vehicle-level SEP-integrated system issues while simultaneously retiring technology risks that cannot be adequately simulated on the ground. The advanced technology utilized by any TDM concept maybe provided through the technology maturation activities projects being conducted by the OCT. These technologies may include but are not limited to high-power Hall thruster propulsion systems, advanced high-voltage solar array systems, and advanced power management and distribution topologies including direct drive. To date, the SEP TDM project has developed a series of seven mission concepts through contracts and Space Act Agreements (SAAs) with industry. These agreements were with the Aerojet Corporation, Analytical Mechanics Associates, Inc., the Ball Aerospace & Technologies Corporation, The Boeing Company, the Lockheed Martin Space Systems Company, the Northrop Grumman Systems Corporation, and Space Systems Loral. The four objectives being addressed by these mission concepts studies were

- Perform an in-space demonstration that advances the maturity of high-power EP technology and high-power solar array power system technology in relevant space environments and operational regimes.
- Demonstrate integrated SEP spacecraft design, fabrication, and test as well as operational modes associated with orbit transfer.
- Demonstrate extensible high-power EP and solar array power system technologies and integrated SEP spacecraft operational modes that can be adapted for use in next-generation, higher power SEP systems.
- Provide a SEP-based transportation capability with performance advancements over those previously demonstrated.
- More details about these mission concepts and the SEP TDM project can be found in the companion paper by Smith et. al.[6]

III. IN-SPACE PROPULSION TECHNOLOGY PROJECT

The NASA Glenn OCT ISP technology program is testing, developing, and maturing high-power Hall thruster technologies that will enable the Agency to achieve its future objectives of robotic and human space exploration. To that extent, in 2011 and 2012,

NASA Glenn high-power Hall development activities and tasks were focused on the following:

- Evaluating performance of existing high-power Hall thrusters (NASA-300M and NASA-457Mv2)
- Developing plasma diagnostics for Hall thrusters
- Performing Hall thruster physics based modeling using the NASA Jet Propulsion Laboratory (JPL) Hall2De code
- Performing Hall thruster structural and thermal modeling
- Designing, fabricating, and testing high-current cathode assemblies with an emission current capability ≥ 100 A and lifetime capability greater than 20,000 hr
- Developing and demonstrating high-power (300 V and ≥ 7 kW) discharge modules for power processing units

The following sections will summarize the results from these activities.

A. High-Power Hall Thruster Testing

The NASA Glenn has a long history of researching and developing high-power Hall thrusters and ion engines. The NASA Glenn's high-power Hall thruster research and development efforts started in 1997 with the award of the T-220 10 kW Hall thruster development contract to TRW, Space Power Inc., and the Keldysh Research Center.[7] The T-220 thruster was fabricated and delivered to NASA Glenn in 1998 and the T-220 underwent extensive performance evaluation and was later subjected to a 1000 hr wear test.[8] In 2000, the In-Space Transportation Program (ISTP) funded the development of two 50 kW class Hall thrusters: one by the Aerojet Redmond Rocket Center and one by the NASA Glenn. The thruster developed by NASA Glenn was designated the NASA-457Mv1.[9] This thruster was tested at power levels up to 72 kW and results revealed key areas in the design that could be improved to increase the performance and reduce mass.[10] A new thruster designated the NASA-457Mv2 was designed and built. Unfortunately, in 2004 the high-power ISTP program was ended and the NASA-457Mv2 performance was never evaluated.[11]

In 2003, NASA's project Prometheus was initiated with the goal of developing nuclear power and propulsion technologies that would enable the exploration of the universe in search of life and resources. The Jupiter Icy Moons Orbiter (JIMO) mission would utilize these newly developed technologies. Mission analysis indicated the optimal high-power EP device for JIMO was a high-power, high-specific impulse Hall thruster. As such the NASA Glenn initiated the development of the NASA-400M.[11] The thruster leveraged and incorporated lessons learned from the design and testing of the NASA-457Mv1. To be able to achieve high specific impulse magnitudes the thruster was designed to operate with krypton propellant at discharge voltages up to ~1000 V. A 300 hour wear test of the thruster indicated that the boron nitride (BN) discharge channel erosion rates were similar to rates measured during the wear test of the T-220.[11,12]

NASA Glenn's long history of developing and testing of high-power Hall thrusters and its world-class vacuum facilities makes it the leading NASA center for developing high-power EP devices. In addition, complete evaluation of previously developed high-power thrusters provides a great start for NASA's effort to develop a high-power SEP stage. As such, under the OCT ISP technology project, the NASA Glenn was tasked with assessing the performance of the existing high-power Hall thrusters that were of interest to SEP TDM and were extensible to the future 300 kW NEO mission. The next two sections will summarize performance evaluation results from recent performance tests of the NASA-300M (20-kW-class) and NASA-457Mv2 (50-kW-class) thrusters.

A.1 NASA-300M 20-kW Hall Thruster

The NASA-300M 20-kW-class Hall thruster was designed, fabricated, and assembled at the NASA Glenn in 2004 and 2005. The NASA-300M was designed and fabricated under the support of the Exploration Systems Mission Directorate (ESMD) Exploration System Research and Technology (ESR&T) program. The NASA-300M design is based on a scaled version of the NASA-457Mv2 and incorporated lessons learned from the development and testing of the NASA-457Mv1, NASA-400M, and NASA-457Mv2 thrusters.[11] The goal of the design was to minimize the size of the design while optimizing the magnetic field and plasma lens to improve performance. The NASA-300M nominal design specifications were discharge power of 20 kW, discharge voltage range up to 600 V, discharge current up to 50 A, and a magnetic circuit that has a similar magnetic field topology as the NASA-457Mv2. The emergence of the ETDD/OCT ISP programs resulted in renewed interest in the NASA-300M.

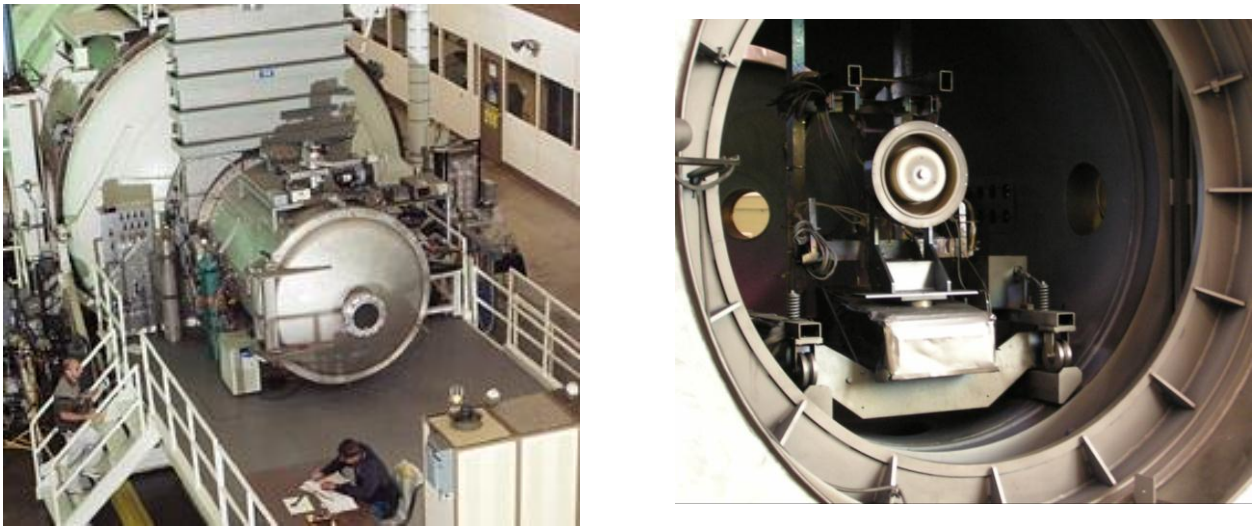

Fig. 1: Photographs of VF5 (left) and the NASA-300M thruster (right) installed in VF5.

Testing of the NASA-300M was performed in vacuum facility 5 (VF5) at NASA Glenn. The VF5 main cylindrical chamber is 4.6 m in diameter and 18.3 m long. Its main port (designated E55) is 1.8 m in diameter and 2.5 m long. The VF5 can be evacuated with cryopanels and oil diffusion pumps. Figure 1 shows a photograph of VF5 and the NASA-300M mounted inside the main port.

Under ETDD, testing of the NASA-300M was performed to discharge power levels up to 20 kW with discharge voltages up to 600 V and discharge currents up to 50 A. Testing was performed with xenon and krypton propellants.[13]

Xenon propellant testing was performed for power levels between 2.5 and 20 kW at 2.5 kW increments. Krypton propellant testing was performed for power levels between 5 and 20 kW in 5 kW increments. Both propellants were tested at discharge voltages between 200 and 600 V. The anode mass flow rate (i.e., discharge current) was varied to attain the prescribed power level at a given discharge voltage; however, the discharge current was not allowed to exceed 50 A due to hollow cathode operational considerations. The cathode flow rate was maintained at approximately 8% of the anode flow rate. Peak facility pressure during thruster operation at 50 A was 2.8×10^{-5} Torr (corrected for xenon). Testing at all power levels and discharge voltage conditions indicated that the thruster operation was stable and no anomalous behavior was observed. In addition, when testing at 20 kW, no thermal limitations on thruster operation were observed. Figure 2 shows a photograph of the thruster while operating on xenon and krypton at 20 kW.

Figures 3 and 4 present the xenon propellant total specific impulse and thrust efficiency results, respectively, for the NASA-300M. These results indicate that the total specific impulse and thrust efficiency increased with increasing power at a given discharge voltage. At 20 kW, NASA-300M

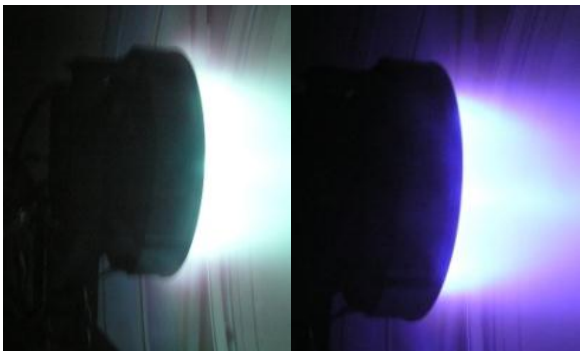

Fig. 2: Photograph of the NASA-300M operating on xenon (left) and krypton (right) at a discharge power level of 20.

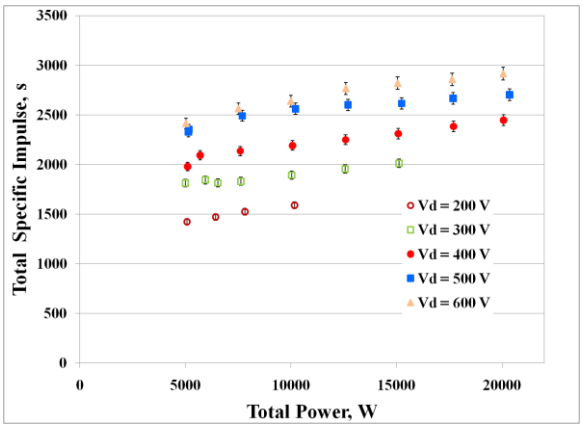

Fig. 3: NASA-300M xenon total specific impulse magnitudes.

performance results indicate that it is able to achieve a peak specific impulse of about 2900 sec at a discharge voltage of 600 V and a peak thrust efficiency of 67% at a discharge voltage of 500 V.

Figures 5 and 6 present the krypton propellant total specific impulse and total thrust efficiency results, respectively. Results in Figures 5 and 6 indicate that, in general, total specific impulse and thrust efficiency increased with increasing power at a given discharge voltage (except for V_d of 200 V). The highest attained total specific impulse and total thrust efficiency were 3223 sec and 63%, respectively, when operating at a discharge voltage of 600 V at 20 kW. Detailed performance evaluation results of the NASA-300M can be found in Reference 13.

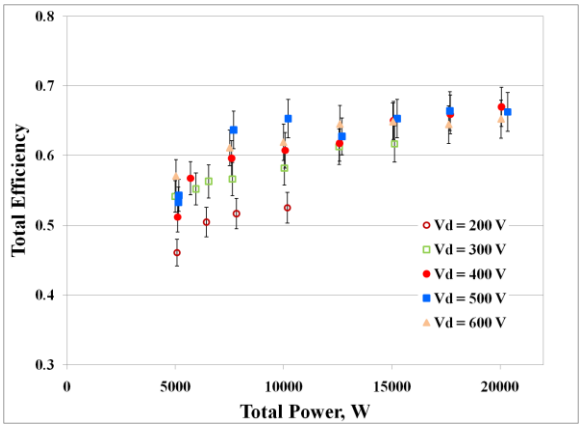

Fig. 4: NASA-300M xenon total thrust efficiency magnitudes.

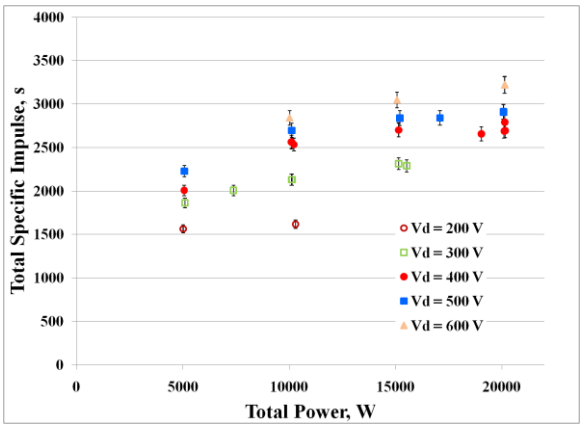

Fig. 5: NASA-300M krypton total specific impulse magnitudes.

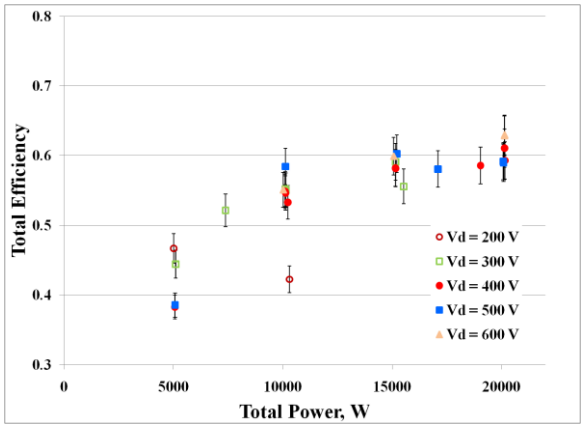

Fig. 6: NASA-300M krypton total thrust efficiency magnitudes.

A.2 NASA-457Mv2 50 kW Hall Thruster

A photograph of the higher fidelity 50 kW Hall thruster (i.e., the NASA-457Mv2), is shown in Figure 7. This high-power thruster has a solid BN discharge chamber with a 457 mm outer diameter and a centrally mounted high-current hollow cathode. The development goal for the NASA-457Mv2 was to advance its technology readiness level from 4 to 5. The fidelity of the laboratory model NASA-457M was improved by addressing thermal and mechanical issues while maintaining the critical features of the laboratory model thruster.[11] The higher fidelity thruster retained the same discharge chamber critical dimensions; however, the magnetic circuit was designed for improved performance and field symmetry. The field topology employed in the NASA 457Mv2 is very similar to that of the laboratory model field, which incorporated the plasma lens topography.[14,15] The centerline radial magnetic field strength was increased by nearly 20% for the same number of amp-turns.[11] The magnetic field produced by the NASA-457Mv2 thruster was measured and compared to its laboratory model predecessor. Although measured magnetic fields for the laboratory model thruster were already reported in References 9 and 16, they were remeasured for

Fig. 7: Photograph of the NASA-457Mv2 thruster.

these comparisons. The measured field strengths of both thrusters were found to be similar.

In addition to the magnetic field circuit, the new mechanical design eliminated deficiencies with respect to anode mounting and electrical isolation, concentricity, and thermally induced mechanical interferences.[11] The thruster's design was assessed using finite element thermal and mechanical modeling techniques. Mechanical analyses assessed vibration tolerance, static deflection, and induced stresses. Thermal models were applied to the mechanical models to predict thermal displacements and corresponding stresses. The thruster's design was updated based on the results of these analyses.

The operating conditions of this performance test are listed in Table 1. Thruster discharge power was varied from 5 to 50 kW over a 200 to 500 V discharge voltage range. The maximum discharge voltage was set by the maximum anticipated specific impulse required by the HEFT mission, which favored values less than about 2600 s to keep mission durations acceptable. A discharge voltage of 200 V was selected as the minimum because of the significant decrease in anode efficiencies as a function of discharge voltage. Performance was measured in 100 V increments; it was also measured at 250 V because of the large change in anode efficiency between the 200 and 300 V cases. Performance was also measured at 350 V to support erosion diagnostics development.

Thrust as a function of total thruster input power is plotted in Figure 8 for the NASA-457Mv2 thruster operating with high anode efficiency. The uncertainty in total power for all results reported herein was estimated to be ±0.3% of the indicated values. The peak thrust demonstrated by the NASA-457Mv2 was 2.3 N at a total thruster input power of 50 kW. The thrust was nonlinear as a function of total input power at the higher power levels at each discharge voltage, which was unlike the laboratory model thruster operating with high magnetic fields.[9,16] This was because the total input power was dominated by discharge power.

Specific impulse as a function of total thruster input power is shown in Figure 9 for the NASA-457Mv2 thruster operating with high anode

Discharge	*Discharge Current, A vs. Discharge Voltage, V*					
Power, kW	*200 V*	*250 V*	*300 V*	*350 V*	*400 V*	*500 V*
5	25 [a]	20	16.7			
6	-	-	-	-	15	
7.5	-	-	-	-	-	15
10	50 [a]	40	33.3	-	25	-
15	75 [a]	60	50	-	37.5	30
20	100 [a]	80	66.7	57.1	50	40
25		100	83.3	-	62.5	50
30			100	85.7	75	60
35				-	87.5	70
40					100	80
45						90
50						100

Table 1: Discharge throttle levels for the NASA-457M v2 thruster performance test.

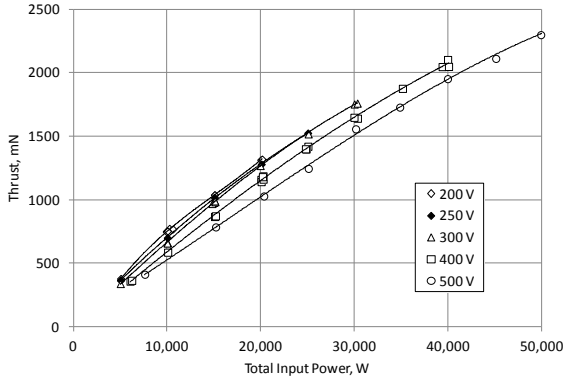

Fig. 8: Thrust as a function of total thruster input power at various discharge voltages for the NASA-457Mv2 thruster operating with high anode efficiency.

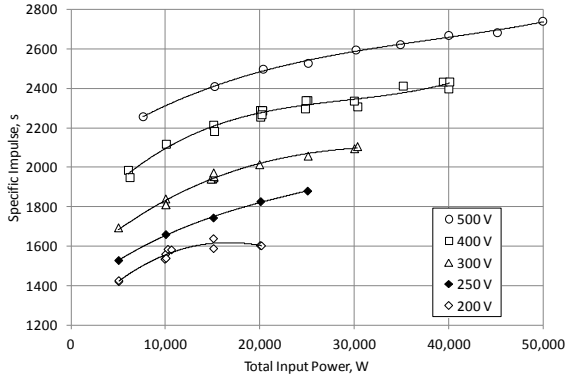

Fig. 9: Specific impulse as a function of total thruster input power at various discharge voltages for the NASA-457Mv2 thruster operating with high anode efficiency.

efficiency. The uncertainty in specific impulse was estimated to typically be ±2.3% of the indicated value. Direct comparisons with the laboratory model thruster were not possible because the laboratory model thruster was operated at fixed cathode flows rather than the 8% of anode mass flow used by the NASA-457Mv2 thruster. The thruster demonstrated specific impulse range of 1420 to 2740 s and also was able to operate at a specific impulse of about 2000 s with a discharge voltage of only 300 V. This is significant because the HEFT trade studies baselined a thruster specific impulse of about 2000 s and lower discharge voltages are typically thought to lead to longer thruster service life capability.[17]

The thrust efficiency as a function of total thruster input power is shown in Figure 10 for the NASA-457Mv2 thruster operating with high anode efficiency. The uncertainty in thrust efficiency was estimated typically to be ±4.2% of the indicated value. As before, direct comparisons with the laboratory model thruster were not possible because it was operated at fixed cathode flows rather than the 8% of anode mass flow used by the NASA-457Mv2 thruster. Regardless, thrust efficiency is dominated by anode performance, and anode efficiencies comparisons were made between the two thrusters in an earlier section. Thrust efficiencies for the NASA-457Mv2 thruster varied from a low of 0.51 at low power to 0.66 at 30 kW with a discharge voltage of 500 V. For a discharge voltage of 300 V, where specific impulses would be about 2000 s, thrust efficiencies varied from 0.57 to 0.63. Detailed performance evaluation results of the NASA-457Mv2 can be found in Reference 18.

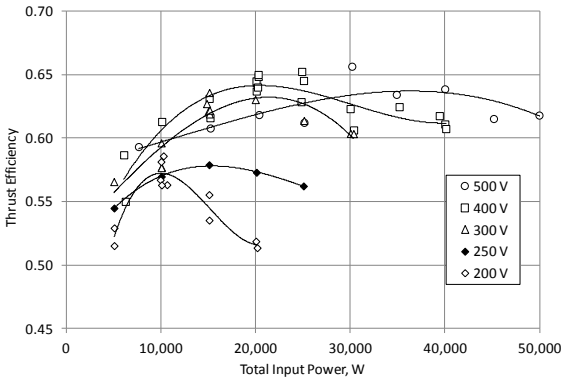

Fig. 10: Thrust efficiency as a function of total thruster input power at various discharge voltages for the NASA-457Mv2 thruster operating with high anode efficiency.

B. Near-Field Plasma Measurements

A number of near-field plasma measurements were taken in order to better understand high-power Hall thruster physics and characterize performance. The purpose of these measurements is to provide data that will help elucidate the physics governing high-power Hall thruster operation and to characterize thruster performance and efficiency. Another purpose is to provide experimental data to validate existing modeling efforts at Glenn and the JPL.[19] The experimental data along with model results will be used to refine thruster design and will help develop a life qualified thruster. This will ultimately lead to the design of a higher performance high-power Hall thruster with a long lifetime at a lower cost.

To reach these goals, an electrostatic probe array was used to measure the near-field plume of the 20-kW NASA-300M and the NASA-457Mv2 from approximately 0.1 to 2 mean thruster diameters ($D_{T,m}$) downstream of the thruster exit plane. Similar measurements have been taken before on the 6-kW H6 Hall thruster at JPL.[20] The probe array consisted of a near-field Faraday probe, a single Langmuir probe, and two emissive probes (one for redundancy). Figure 11 shows a photograph of the electrostatic

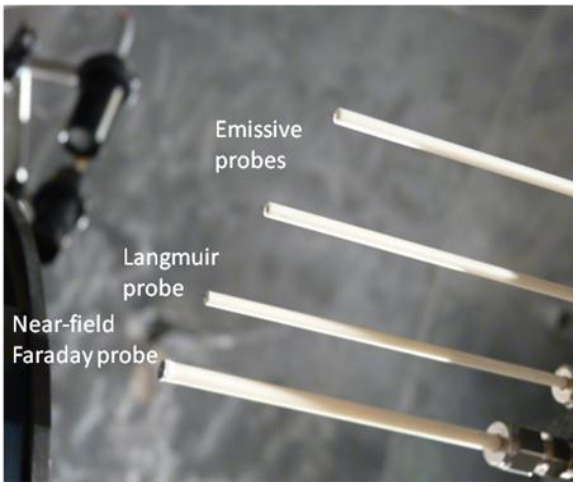

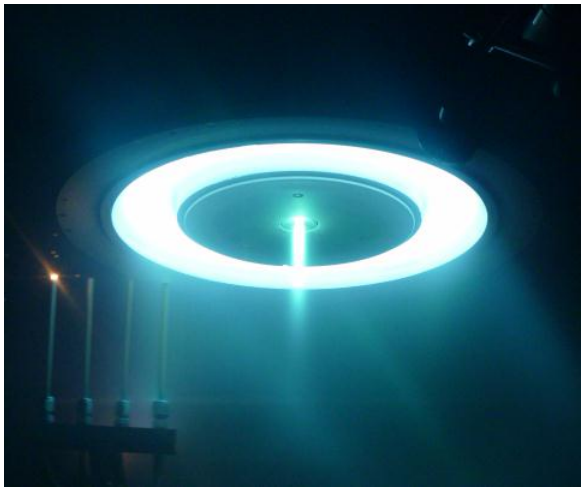

Fig. 11: Photographs of the probe array used in this study. Left: Photograph showing order of four probes within array, prior to operation. Right: Array sweeping near the thruster exit plane of the 300M (array is shown to the left of thruster).

probe array. Measurements at these distances were facilitated by a high-speed linear motion table typically run between 250 and 375 mm/s, helping to ensure probe survivability in the harsh near-field environment. In addition, optical emission spectroscopic measurements were also performed. The next two sections will highlight findings from those studies.

B.1 Ion Current Density Measurements

Ion current density plume measurements provide an accurate estimate of the plume divergence in a Hall thruster. These measurements are typically performed with a Faraday probe (see Fig. 11). Details of the probe design, motion table setup, and the data acquisition electrical circuit setup is detailed in References 21, 22, 23. For this test, the NASA-300M was operated at seven conditions spanning discharge voltages from 200 to 500 V, discharge currents from 20 to 67 A, and discharge powers of 10 and 20 kW. The nominal operating condition was 500 V and 40 A. The BN channel walls of the NASA-300M were largely un-eroded for this present test. These channel walls have accumulated at most 70 hr prior to the start of the tests described in this section.

For this test, the NASA-457Mv2 was operated at 14 conditions spanning discharge voltages of 200 to 500 V, discharge currents of 40 to 100 A, and discharge powers of 10 to 50 kW. The nominal operating condition was 500 V and 100 A. The anode efficiency of the NASA-457Mv2 varies from 55 to 70% over the tested operating conditions. The test matrixes of the near-field Faraday probe test were chosen to target a variety of discharge voltages in order to characterize the thrusters for both high thrust-to-power (low specific impulse) and high specific impulse operation. Many of the conditions chosen also enable constant-current and constant-power trend studies. Figure 12 shows a diagram of all operating conditions tested for the present study for both the NASA-300M and the NASA-457Mv2.

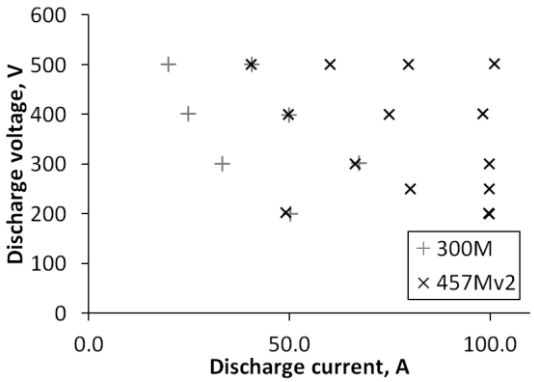

Fig. 12: Operating conditions for the ion current density measurements for the NASA-300M and NASA-457Mv2 thrusters.

To aid in the creation of the data location matrix, predicted near-field plume characteristics were drawn from a Hall2De simulation study on the NASA-300M performed by Mikellides, et al.[19] From prior tests on other Hall thrusters of similar design, some ion acceleration was expected to take place downstream of the exit plane. Thus, the axial spatial resolution of the ion current density data is highest in the region nearest the thruster channel exit. The spatial resolution decreases as the probe travels axially away from the thruster. The spacing is based on the predicted plasma density and the assumption that changes in the plasma should become more gradual as the plasma density falls. The data location matrix

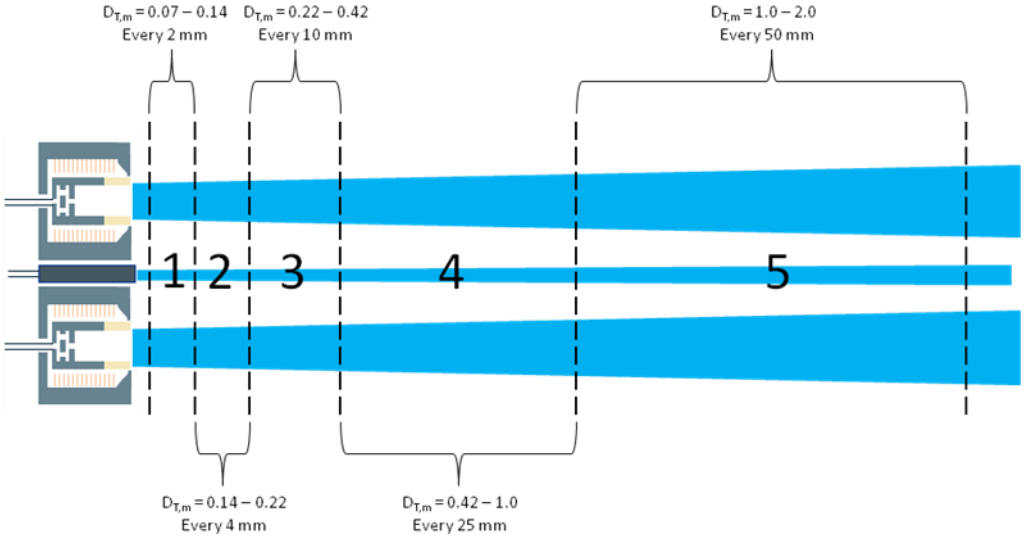

Fig. 13: A diagram of the spatial resolution of radial sweeps taken for the NASA-300M and NASA-457Mv2.

for the NASA-457Mv2 was created based on geometric scaling from that of the NASA-300M. Figure 13 (previous page) shows a diagram of the spatial resolution of the radial sweeps for the NASA-300M and NASA-457Mv2 thrusters.

Figures 14 and 15 present typical NASA-300M ion current density profiles and a contour map at 500 V and 20 kW. Additional NASA-300M and NASA-457Mv2 ion current density profiles and contour maps can be found in Reference 21. Total ion current and divergence angles were calculated based on the methodology described Reference 21. For each operating condition, calculations were carried out for each of the 1-e, 2-e, and 3-e integration limits. The reported divergence angle is calculated from the radial position of the point of origin up to the outer integration limit. Thus, the reported angle is strictly an outer-side divergence angle. Table 2 shows a summary of the results from carrying out total ion current and outer-side divergence angle calculations for the NASA-300M and NASA-457Mv2 thrusters. The first five columns of the table list basic operating parameters including thruster, discharge voltage, discharge current, anode mass flow rate, and Faraday probe bias voltage, which is measured with respect to the facility ground. The sixth and seventh columns list the total ion current integrated within the 1-e limits and 2-e limits, respectively. The eighth and ninth columns list the outer-side divergence angle calculated within the 1-e limits and 2-e limits, respectively. Calculations with 3-e limits were carried out but are not shown because the resulting total ion current varied from 83 to 92% of the discharge current, these were deemed too large to be

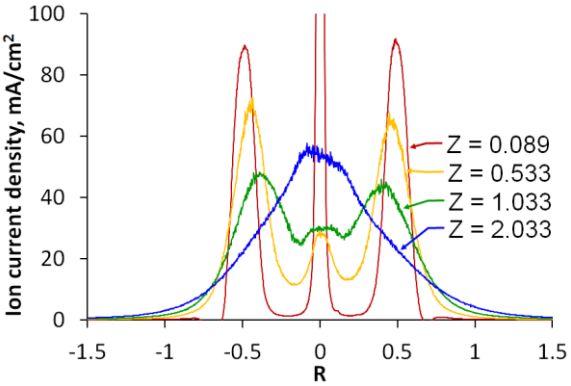

Fig. 14: Ion current density profiles for the NASA-300M operating at 500 V, 40 A.

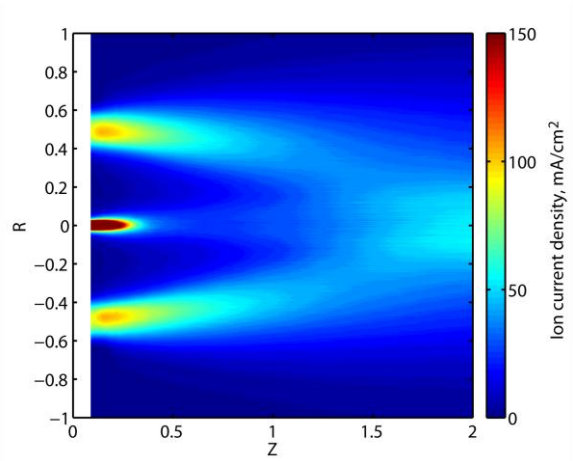

Fig. 15: Flooded contour of ion current density for the NASA-300M operating at 500 V, 40 A.

real. For 1-e and 2-e limits, this percentage is 63 to 75% and 78 to 87%, respectively. For state-of-the-art Hall thrusters, this percentage is typically 70 to 80%,[24,25,26,27] so the correct choice of integration limit appears to lie somewhere between 1-e and 2-e. Since no further information is available to help determine the right integration limits, both 1-e and 2-e values are reported.

One very notable feature of the outer-side divergence angle result is how small they are compared to typical far-field measurement results. Reducing far-field ion current density data typically yield divergence angles in the range of 15° to 25° for state-of-the-art Hall thrusters.[25,28] Yet, the above near-field measurement show that the discharge beam exits the thruster with an average of 4° and 8° divergence as calculated with the 1-e and 2-e limits, respectively. Lastly, a short study of the NASA-457Mv2 plume while roughly doubling the magnetic field strength reveal that the overall plume shape does not change greatly but the cathode plume becomes more distinctly separated from the overall plume structure. While the anode mass flow rate was increased by about 9% to keep the discharge current constant, the total ion current increased by approximately 5% when operating with the higher magnetic field strength.

	V_d, V	I_d, A	Mass flow, mg/s	Probe Bias, V	Total ion current, A		Outer-side divergence angle, deg.	
					1-e limits	2-e limits	1-e limits	2-e limits
300M	200	50.3	39.9	-60	37.2	42.7	6.3	12.4
	300	33.3	32.3	-60	22.6	27.6	1.9	4.7
	301	67.3	52.2	-60	45.0	52.8	3.6	9.3
	401	24.9	25.2	-60	17.2	20.9	2.0	4.9
	399	50.0	43.8	-60	33.9	40.9	1.8	4.7
	501	19.9	20.7	-60	14.4	17.1	2.9	5.7
	501	40.6	37.4	-60	28.6	33.8	2.9	5.8
457Mv2	202	49.1	46.1	-60	31.0	38.3	4.1	7.3
	200	99.8	77.8	-60	71.0	82.1	8.1	14.9
	250	80.2	66.4	-60	54.8	66.4	4.7	9.2
	250	99.8	76.7	-60	66.1	78.7	4.8	10.2
	301	66.4	59.7	-60	44.1	54.3	3.5	6.1
	300	99.8	79.5	-60	72.9	86.4	5.2	9.7
	400	49.7	48.4	-60	33.7	41.8	3.1	5.8
	400	74.8	65.9	-60	51.9	63.1	3.5	5.7
	401	98.2	79.1	-90	68.2	82.4	4.3	6.9
	501	40.5	38.8	-80	28.9	34.7	4.0	6.9
	500	60.1	56.6	-80	41.6	50.9	3.0	5.5
	501	79.7	69.0	-80	56.7	67.9	3.7	6.4
	501	101.1	80.5	-90	73.5	87.8	4.4	7.3
hi-mag	201	99.6	84.9	-60	74.6	86.4	8.7	15.9

Table 2: Summary of total ion current and outer-side divergence angle analysis.

B.2 Plasma Potential Measurements

Plasma potential measurements were performed with an in-house designed and built emissive probe (shown in Fig. 11). Details of the probe design and the electrical circuit used during data acquisition are provided in References 22 and 23. For the NASA-300, plasma potential measurements were performed at 20 kW and 500 V operating condition. Figure 16 shows the contour of the of plasma potential at this operating condition. It is evident from the figure that the plasma potential is fairly uniform throughout most of the near-field plume. Most of the acceleration zone that was captured lies within 0.2 $D_{T,m}$ of the thruster exit, while the remainder of the plume is at 20 to 30 V above cathode potential. The maximum measured plasma potential at 0.1 $D_{T,m}$ from the exit plane is approximately 96 V. This confirms that while near-field plume studies provide critical information about the plasma just downstream of the exit plane, internal measurements are necessary to capture the majority of the acceleration zone.

For the NASA-457Mv2, plasma potential contours are shown in Figure 17. It shows that most of the near-field plume is at a fairly uniform potential of approximately 20 to 25 V above cathode potential for both operating conditions. Most of the acceleration zone appears to be contained within 0.4 $D_{T,m}$ of the thruster exit plane. The maximum measured plasma potentials at 0.08 $D_{T,m}$ from the exit plane are 52 V at 300 V and 30 kW and 55 V at 400 V and 30 kW. This confirms that while such near-field studies provide critical information regarding the plasma downstream of the exit plane, the majority of the acceleration zone lies upstream of this region and requires internal measurements to fully capture it. From Figure 17, the plasma potential appears to

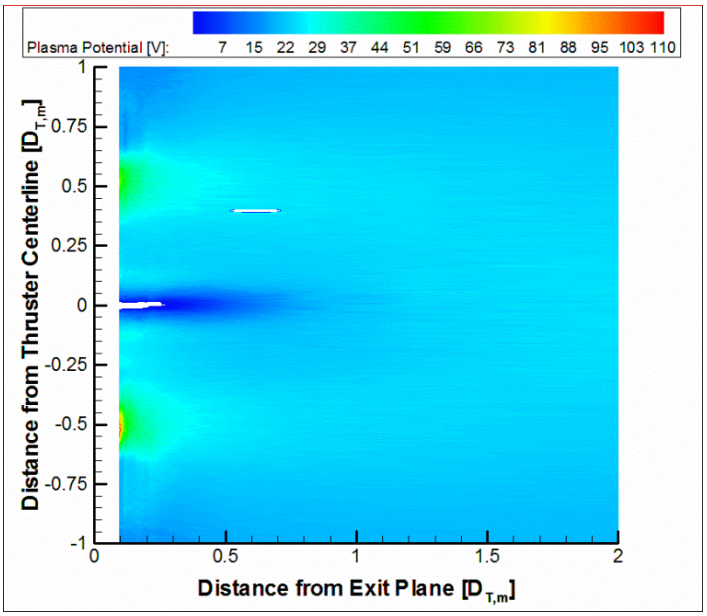

Fig. 16: Contour map of plasma potential in the near-field plume at 500 V and 20 kW. Most of the acceleration zone captured is within 0.2 $D_{T,m}$ of the thruster exit plane. All values reported are with respect to cathode potential.

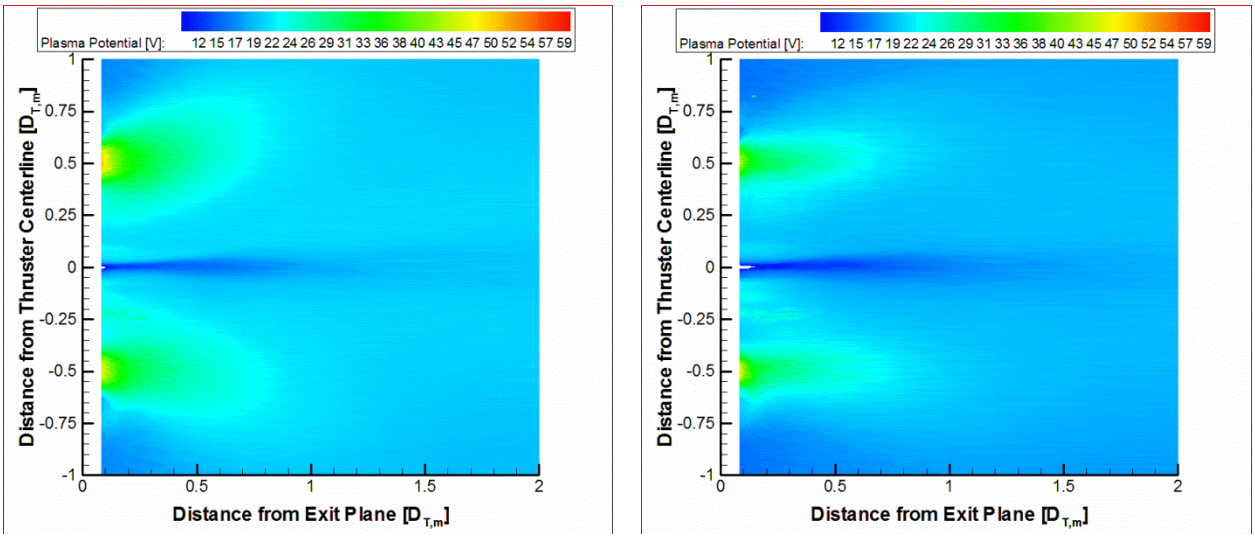

Fig. 17: Plasma potential contours in the near-field plume of the NASA-457Mv2. Left: 300 V at 30 kW. Right: 400 V at 30 kW. The acceleration zone for both conditions appears to be contained within 0.4 $D_{T,m}$ of the thruster exit plane. All reported potentials are with respect to cathode potential.

drop off radially from channel centerline more rapidly at 400 V compared to 300 V. This is an indication that the plasma is more concentrated around channel centerline at 400 V, thus implying the beam is more collimated. This trend is confirmed with ion current density measurements made in the near-field at these conditions.[5]

Detailed discussions of the plasma potential results of the NASA-300M and NASA-457Mv2 are provided in References 22 and 23, respectively.

B.3 Electron Temperature Measurements

Electron temperature measurements were performed with an in-house NASA Glenn designed and built single Langmuir probe (shown in Fig. 11) that was housed inside a double-bore alumina tube. An identical wire was sleeved in the adjacent bore and encapsulated by high-temperature Ceramabond. A "null" probe was biased in the same manner as the "active" probe, but since it was isolated from the plasma, it was used to characterize the capacitive

currents in the electrical lines that can be subtracted out during plasma processing and reduction. Data analysis of the Langmuir probe I-V characteristics followed the simple Langmuir probe theory.[29,30] Details of the probe design, raw data analysis procedures, and the electrical circuit used during data acquisition are provided in References 22 and 23.

The near-field NASA-300M electron temperature profiles were obtained for various discharge voltage and power operating conditions. In Reference 22, results are presented for discharge operating conditions of 300 V and 10 kW, 300 V and 20 kW, 400 V and 20 kW, and 500 V and 20 kW. Results presented in this paper are for operation at a discharge voltage of 500 V and 20 kW. Figure 18 left shows that the high temperature region is contained within 0.3 $D_{T,m}$ of the thruster exit plane. Afterwards, the electron temperature is fairly uniform in the near-field at 2 to 5 eV. The maximum measured electron temperatures at 0.07 $D_{T,m}$ from the exit plane were 27 eV at 500 V and 20 kW. As reported in Reference 22, higher electron temperatures are expected at higher discharge voltages due to increased ohmic heating. In addition, changes in the location of the ionization and acceleration zones introduce additional factors that affect the maximum electron temperature seen in the near-field plume. Detailed discussion of the electron temperature measurements at the various operating conditions of the NASA-300M was presented in Reference 22, but in general, the results indicate that there exists a lobe-like structure that is strongly reminiscent of the magnetic field topology in the near-field region of the NASA-300M.

For the NASA-457Mv2, electron temperature profiles were obtained for various discharge voltage and power operating conditions. In Reference 23, results are presented at discharge operating conditions of 300 V, 400 V, and 500 V at 30 kW, and 500 V at 50 kW. Figure 18 (right) shows the electron temperature contours at 500 V and 50 kW. For all operating conditions, the region of high temperature is contained within 0.25 $D_{T,m}$ from the thruster exit plane. The remainder of the near-field plume is at roughly constant temperature ranging from 2 to 5 eV. The maximum measured electron temperatures at 0.06 $D_{T,m}$ from the thruster exit plane are 26 eV for 300 V at 30 kW, 24 eV for 400 V at 30 kW, 27 eV for 500 V at 30 kW, and 32 eV for 500 V at 50 kW. The NASA-457Mv2 electron temperature contours at 500 V are very similar to results found for the NASA-300M.

Finally, both the NASA-300M and NASA-457Mv2 electron temperature contours provided great insights as to the location and structure of the acceleration zone, but detailed probing of the discharge chamber is required to assess and determine the precise location of the acceleration zone and lifetime of the thruster. As is highlighted in section B.5, measurements of the floating potential, electron temperature, and number density were performed on the NASA-300M thruster. At the present time, there are no plans to perform such measurements on the NAS-457Mv2, but if that need arises such measurements could be performed using the existing setup.

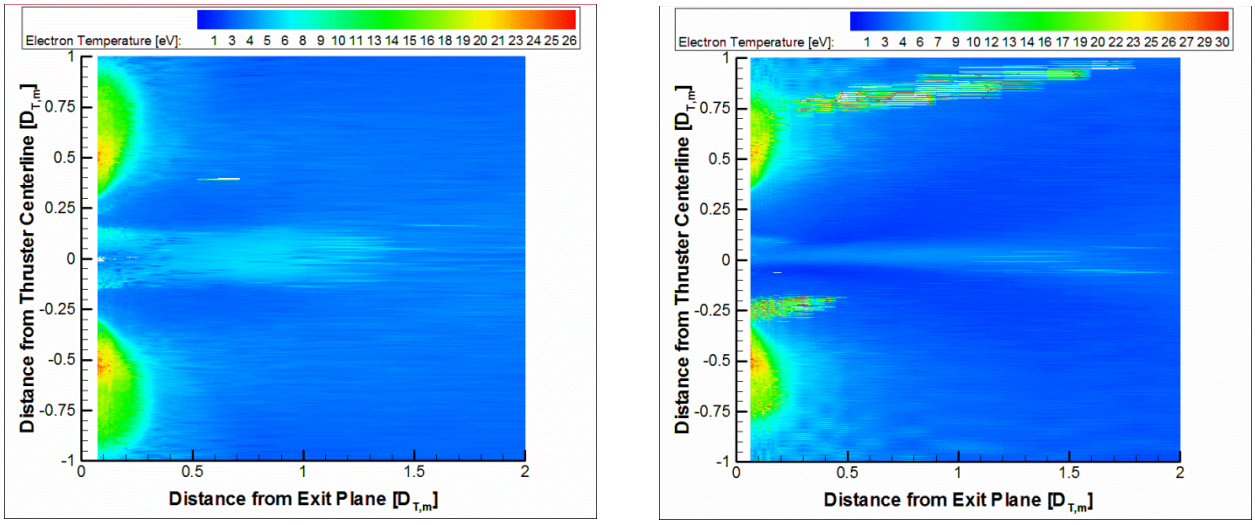

Fig. 18: Contour maps of electron temperature in the near-field plume of the NASA-300M and NASA-457Mv2. Left: NASA-300M at 500 V and 20 kW. Right: NASA-457Mv2 at 500 V and 50 kW. The two thrusters contour profiles exhibit similar structure in their isothermal lines.

B.4 Optical Emission Spectroscopy

Another goal of the advanced plasma diagnostics development under the OCT ISP technology project is to demonstrate nonintrusive diagnostics capability that can assess thruster life under various operating conditions. The ultimate goal is to demonstrate and integrate a nonintrusive diagnostic capability that provides a real-time erosion measurement that mitigates or eliminates the need for very long duration testing of developmental hardware (at least from a life-limiting wear perspective). The technique will have the potential to measure not only insulator erosion but also cathode surface erosion and efflux of cathode emitter material. It may also have the ability to characterize the interaction of the thruster plume with spacecraft surfaces. The following summarizes the first phase in the development of this capability, which now has the ability to provide a real-time assessment of the relative insulator erosion rate with thruster operating condition.

The evaluation and demonstration of the optical emission spectroscopy (OES) erosion monitoring technique took advantage of opportunities to test with different Hall thrusters. In addition to providing erosion data on these different thrusters, the ability to use the technique with a variety of thrusters of significantly different powers was demonstrated. One objective of this investigation was to compare the erosion trends of the small, albeit High Voltage Hall Accelerator (HiVHAc) engineering development unit (EDU) thruster with the higher power NASA-300M and NASA-457Mv2 thrusters. All thrusters operated on xenon propellant in either vacuum facility 8 (VF8) or VF5 at NASA Glenn. Magnetic field settings were selected to optimize performance of each thruster.

The use of fiber optic probes to characterize the wear and operation of high-power Hall thrusters has been demonstrated. Figure 19 shows a photograph of the testing configuration. The emission of boron atoms has been normalized (NB values) using an actinometrical method that mitigates the need to know the electron temperature in the discharge or the detailed excitation and quenching mechanisms of the boron I transitions. The technique yielded a real-time, nonintrusive diagnostic that captured trends in BN insulator erosion as various thrusters were operated. In this regard, it demonstrated the ability to provide at least a real-time relative assessment of the impact of changes in the operating conditions. Also, the clear differences in $I_{B,250}$ (intensity of a boron transition with wavelength of 250 µm) collected from probes focused a few millimeters apart on the BN walls demonstrated the ability to measure with spatial resolutions on the order of a few millimeters within the thruster.

Gold and silver foil layers were used to demonstrate the potential of the OES technique incorporating actinometry. While not directly applicable to the life assessment of the thruster itself, the technique demonstrated the ability to correlate the OES signal with the overall erosion rate of the target materials. Note that there is qualitatively good agreement. Thus, the technique demonstrated the ability to measure BN erosion rates if those rates can be correlated with $I_{B,250}$.

Insulator erosion trends characterized by the normalized boron neutral atom spectral emission at 250 nm were obtained on the 3.9 kW HiVHAc EDU thruster, the 20 kW NASA-300M thruster, and the 50 kW NASA-457Mv2 thruster. The NB values were

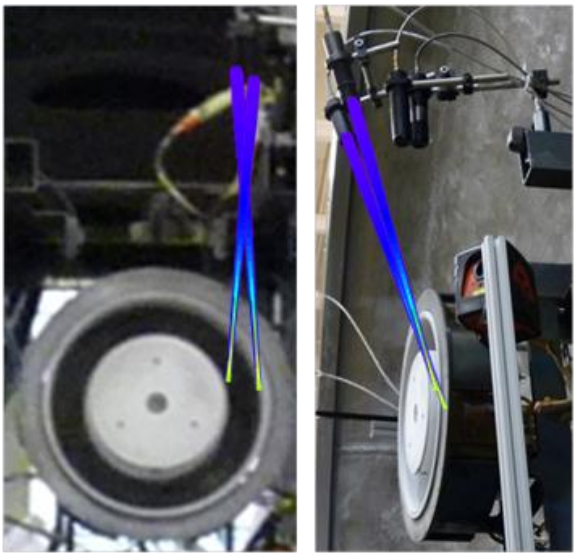

Fig. 19: Superposition of the sampling volume onto the test configuration of the NASA-300M. Note that the regions of relatively high sampling (red-green regions) are in the plume and the regions of lower sampling are largely outside of it.

linearly proportional to power and discharge voltage for the HiVHAc thruster and showed little difference between the inner and outer walls as seen in Figure 20. NB values for the NASA-300M thruster showed a greater than linear dependence on power, primarily trending with discharge current. The inner wall of this thruster had much higher NB values than the outer wall. NB values of the NASA-457Mv2 thruster also showed an unexpected dependence on discharge current as illustrated in Figure 21. The NB values varied linearly with discharge current with a slope roughly equal to (1-ηA). Why a stronger dependence on discharge voltage was not observed for the high-power thrusters remains unclear but may result from the averaging of the xenon lines by the OES probes used to normalize (correct) the raw $I_{B,250}$. More analysis and data are required to confirm these trends or to resolve why the OES technique is not capturing the proper dependence of the erosion rate on the operating condition. Details of the OES technique development can be found in Reference 31.

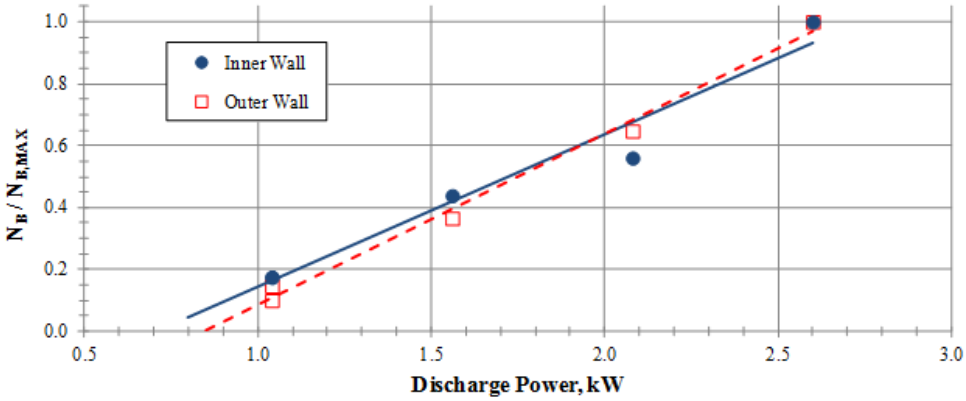

Fig. 20: Variation in N_B normalized to its maximum value for the HiVHAc EDU thruster operating at a discharge current of 5 A.

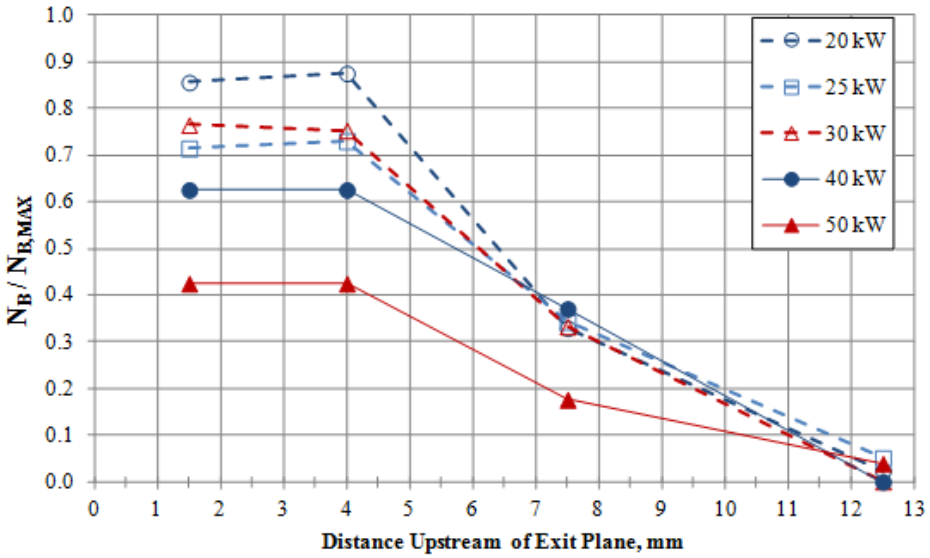

Fig. 21: Trends in normalized N_B values as a function of axial location for 100 A operation of the NASA-457Mv2 thruster. Note that the signal decreases for increasing V_d.

C. Far-Field Plume Measurements

Far-field plasma measurements were performed within the far-field plume of the NASA-300M Hall thruster. Data were collected up to 500 V discharge voltage and 20 kW discharge power. The far-field measurements incorporated the use of a Faraday probe, Langmuir probe, a retarding potential analyzer (RPA), and an E×B probe shown on the photograph in Figure 22 as mounted in VF5. Spatial mappings of the beam current density, as well as single point measurements of the ion charge state and acceleration potential were made. Measurements were performed to gain insights into the various efficiency losses associated with Hall thrusters and how they vary with operating conditions. In addition, the far-field measurements provide valuable insights into the thruster/spacecraft interactions. The measured plasma properties will be used to evaluate how the plume from high-power Hall thrusters interact with the various spacecraft surfaces. The far-field data is being analyzed and will be presented at the 2013 International Electric Propulsion Conference (IEPC 2013).

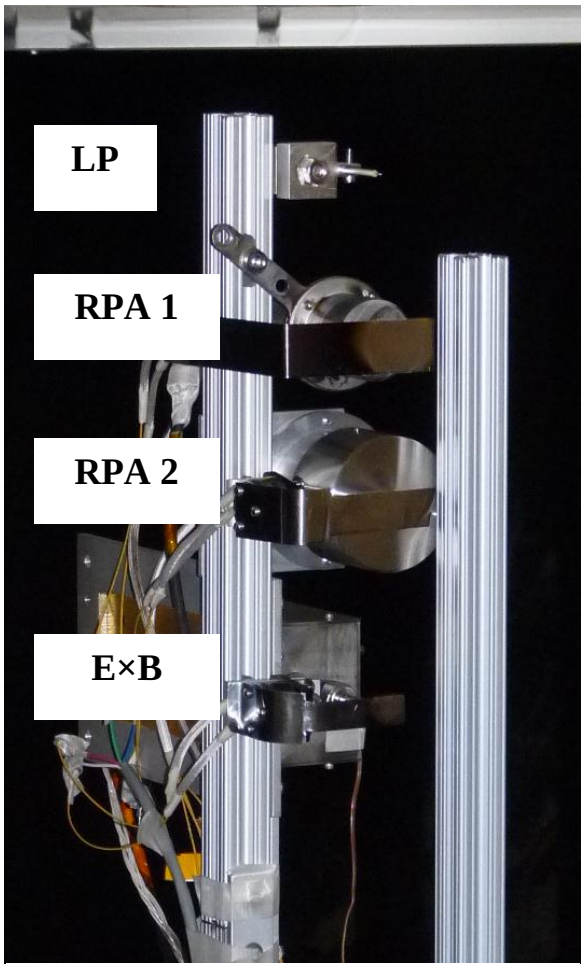

Fig. 22: Photograph of the far-field probes.

D. Internal Discharge Chamber Plasma Measurements

Internal discharge chamber plasma measurements were obtained for the NASA-300M. The test provides critical reference data for attaining a better understanding of high-power Hall thruster physics, provides data for validating/improving a JPL Hall thruster simulation code, and will help guide the design of future high-power, long-life, and high-performing Hall thrusters. Additionally, the newly assembled plasma diagnostics setup enhances NASA Glenn's plasma diagnostic capabilities for future EP testing.

Tests were performed in VF5. The tests were carried via a newly developed high-speed axially reciprocating probe (HARP) system that can rapidly inject and retract probes from the channel of the Hall thruster. Figure 23 shows a photograph of the setup inside VF5.

For this test series the NASA-300M was operated at five different conditions spanning discharge powers of 10, 15, and 20 kW, and discharge voltages of 300, 400, and 500 V. These operating conditions cover the power and specific impulse range of interest to OCT missions. Floating potential, electron temperature, and number density measurements were performed at various radial locations inside the NASA-300M discharge chamber. Initial data inspection revealed that the data will provide great insights as to the location of the ionization and acceleration zones and will be critical in validating the JPL Hall2De code. Data analysis of the acquired data is ongoing and results will be presented in an upcoming paper. The internal, near-field, far-field data, thruster performance, and numerical modeling results will greatly enhance our understanding of high-power Hall thruster physics and lifetime and will contribute to future design of high-power and high- fidelity Hall thrusters.

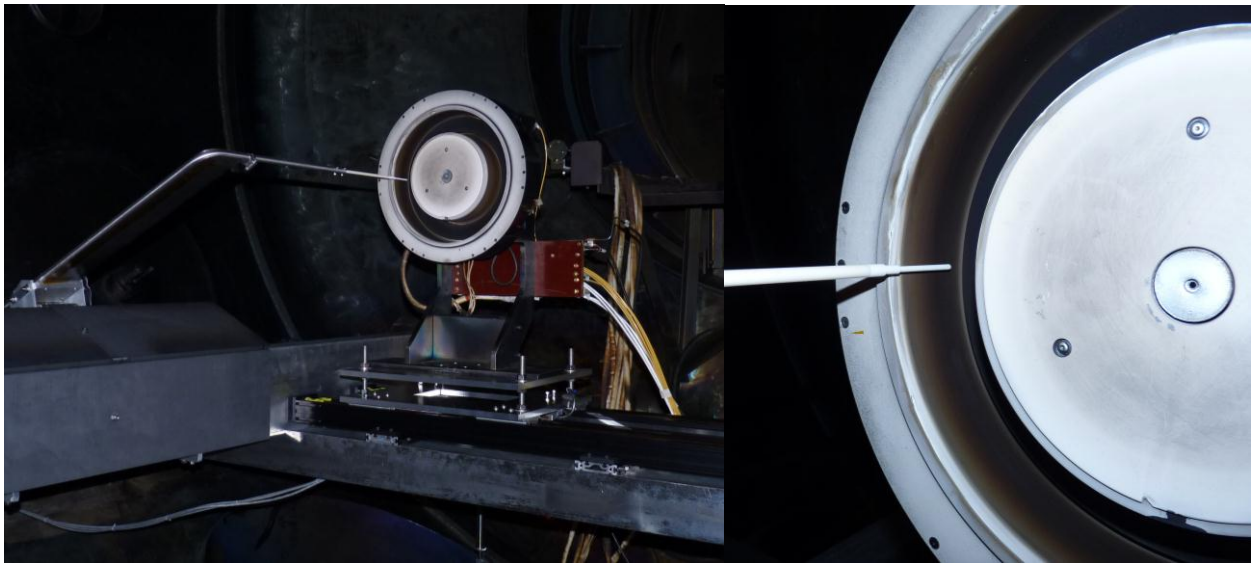

Fig. 23: HARP stage setup inside VF5 with NASA-300M 20 kW thruster.

E. Physics Based Modeling

To reduce flight risk as well as time and cost during the development and flight qualification of high-power Hall thrusters, NASA JPL and Glenn are employing physics-based numerical simulation, plasma and wear diagnostics, and thruster testing by combining unique capabilities at the two centers.

A first series of numerical simulations of a 20-kW class Hall thruster have been completed to establish the groundwork for the development of high-power, high-performance, and long-life Hall thrusters. The numerical simulations have been performed with Hall2De, a two-dimensional axisymmetric, magnetic-field-aligned computational mesh (MFAM) plasma solver developed at NASA JPL.[32,33] Detailed results from the computational work were presented in Reference 19. Simulation results provided a first assessment of the erosion rates in the design of the NASA-300M. Figure 24 shows the two-dimensional contours of the number density in the thruster's acceleration channel. The simulation results indicated that the ionization zone is located far upstream of the channel exit and that significant ion focusing is achieved due largely to the applied magnetic field topology. This combination leads to erosion rates along the channel insulators that do not exceed 1 mm/kh. Recent findings on erosion physics and related wear mitigation techniques suggest it may be possible to modify the magnetic circuit and channel geometry of this thruster to achieve magnetic shielding, a technique that seeks to reduce erosion rates at the channel walls by more than one order of magnitude. Reduced erosion rates are attained by modifying the thruster's magnetic circuit to reduce ion bombardment on the discharge channel walls.[32,33] Recent simulations have been performed on a magnetically shielded version of the NASA-300M thruster. Extended simulations that include assessment of thermal loads to the thruster surfaces, plasma diagnostics and model validation, thruster modifications, and testing constitute the focus of this effort in the near future.

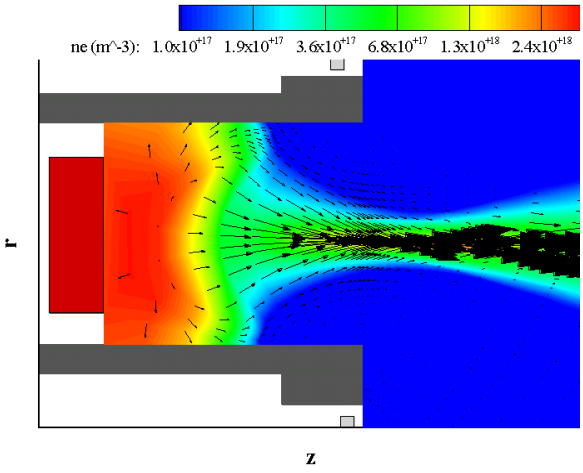

Fig. 24: Two-dimensional contours of the number density in the NASA-300M discharge channel.

F. High-Current Hollow Cathode Development

As part of the OCT ISP technology project, the NASA Glenn is developing and testing new high-current hollow cathode assemblies that can meet and exceed the required discharge current and life-time requirements (≥20,000 hr) of high-power Hall thrusters test results of three high-current hollow cathode configurations were reported in Reference 34. Figure 25 shows a photograph of configurations 1 and 2. Test results indicated that both configurations were able to attain lower peak emitter temperatures compared to state-of-the-art hollow cathode assemblies. Figure 26 compares the cathode orifice plate tip temperatures for configurations 1 and 2 at 50 A and 100 A. Test results at 100 A and a xenon flow rate of 37 sccm indicate that configuration 2 cathode orifice plate tip temperature is 70 °C lower than that for configuration 1. Also, comparing configurations 1 and 2 cathode orifice plate tip temperatures at 100 A to test results of previously tested high-current cathode configurations at NASA Glenn shows that configurations 1 and 2 cathode orifice plate tip temperatures were 200 to 270 °C lower than what was measured by Carpenter et al. in 2001[35] and were approximately 100 to 170 °C lower than what was measured by John et al. in 2005.[36] Configuration 2 cathode orifice plate tip temperature of 1132 °C at 100 A is consistent with the temperature magnitude that is required for emitter life exceeding 20,000 hr. A preliminary analysis of configuration 2 test results indicated that a uniform emitter temperature was realized along the emitter surface. This results in uniform impregnate deletion rates across the emitter and long life.[34]

Near-term tests will include operating configuration 2 for extended durations. In addition, detailed emitter temperature and plasma measurements inside the hollow cathode emitter region have to be performed. These measurements will be supplemented by extensive physics-based hollow cathode modeling.

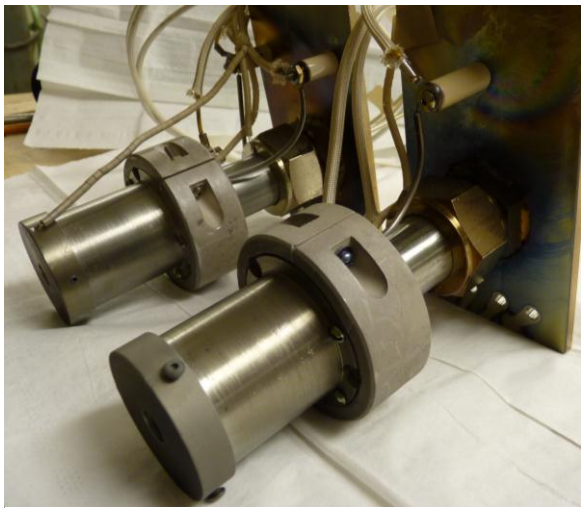

Fig. 25: Photograph of high-current hollow assemblies configurations 1 and 2.

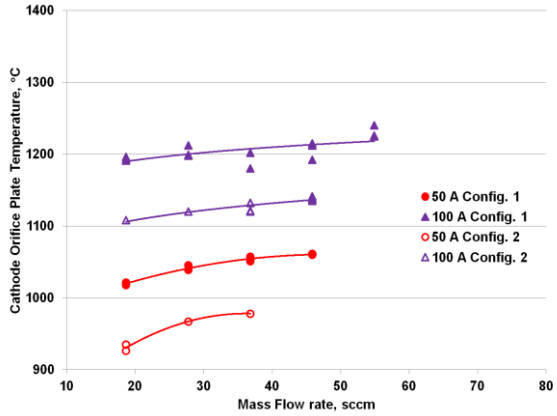

Fig. 26: Configurations 1 and 2 cathode orifice plate tip temperature variation with flow rate for discharge currents of 50 and 100 A.

G. Thermal and Structural Modeling of High-Power Hall Thrusters

Thermal modeling of the NASA-300M and NASA-457Mv2 thrusters was performed to gain insight into their thermal characteristics and to improve future designs of flight thrusters. The models were created using commercially available software. Simulations were performed for the thruster operation under deep space cold conditions and under worst-case hot conditions—in low Earth orbit with solar and Earth albedo heat fluxes while firing. In addition, simulations were also performed for a ground test environment to evaluate the model results against experimentally measured values. Both the NASA-300M and NASA-457Mv2 were instrumented with thermocouples during performance and plume testing to provide experimental data for model correlation. Figures 27 and 28 plot the experimental temperature data with the thermal modeling results for the NASA-300M and NASA-457Mv2 thrusters, respectively. Since the data were not obtained from dedicated thermal characterization tests, but simply the temperatures collected during performance and plume testing, thermal steady state was not achieved for all of the test data. Curve fits to the semi-empirical estimates of the steady state temperatures based on the experimental data are also shown in Figsures 27 and 28. Simulation results indicate a fair comparison to the steady state temperature curves.

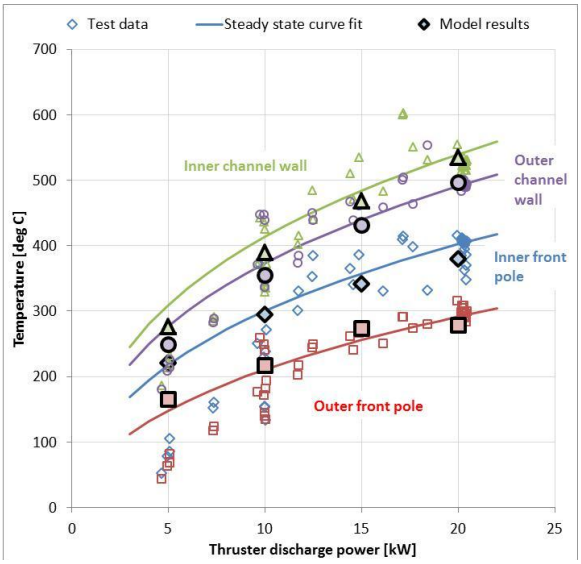

Fig. 27: Test temperatures, including steady state curve fits, and model results for the NASA-300M Hall thruster.

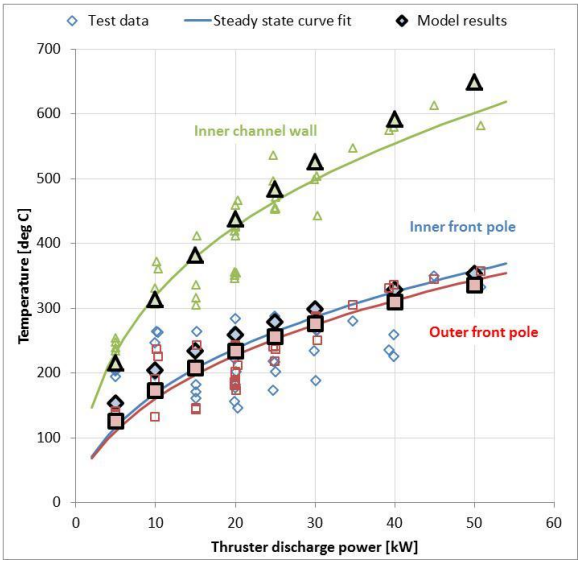

Fig. 28: Test temperatures, including steady state curve fits, and model results for the NASA-457Mv2 Hall thruster.

Structural modeling of the NASA-457Mv2 Hall thruster was also performed with commercially available software to evaluate the response of the thruster under launch acceleration and vibration loads. The calculated stresses of the thruster components were well within material margins. A preliminary assessment of thermally-induced stress was also performed with inputs from the thermal modeling results. The primary thruster modes were also evaluated. The NASA-457Mv2 thruster, designed to incorporate structural improvements over the previous version, will undergo vibration testing at NASA Glenn to provide data to correlate to the modeling efforts. The lessons learned from the thermal and structural analyses and testing will aid in the understanding and improvement of existing thruster designs and also provide guidelines for future thruster development.

H. High-Power Discharge Module Development for High-Power Hall Thrusters

The development of a high-power SEP system for HEOMD missions will require the development of power electronics. As power level increases, it becomes more difficult to develop the power converters because of component availability, the increase in current stress, and conduction losses. The increase in power level impacts not only the EP system but also the power management and distribution (PMAD) systems and the solar arrays. For future high-power spacecraft, it may be advantageous to implement high- voltage power systems to mitigate these effects. However, one issue with this implementation is that space qualified, radiation-hardened, and high-voltage semiconductors are very scarce. Since part qualification will likely be necessary for a power processing unit (PPU) with high power, consideration of emerging semiconductor technologies like silicon carbide (SiC) and gallium nitride (GaN) should be made. Recently, practical commercial transistors became available for both of these technologies. SiC is especially appealing for high-power applications because the available devices are rated for high voltage (1200 VDC) and should also have good immunity to radiation effects.

A comprehensive trade study was conducted to look into a variety of semiconductor technologies and transistor devices for development of a high-power PPU. Models to estimate performance and power losses as a function of converter topology, voltage, current, and frequency were generated. The models were validated with data from component testing. SiC metal oxide semiconductor field effect transistors (MOSFETs) were selected as the best candidates for high-power PPUs with input voltages higher than 200 V. SiC Schottky diodes were selected for high-voltage, high-current rectification.

The effort then focused on designing and building a high-power module to process power for a Hall thruster main discharge. A breadboard module is shown in Figure 29. An input voltage of 300 V ± 10% was chosen for this design anticipating it would operate of a high-voltage power bus. An output voltage range of 300 to 400 V was chosen because it will result in a specific impulse that would satisfy most missions of interest. The module was designed to process as much power as possible while meeting

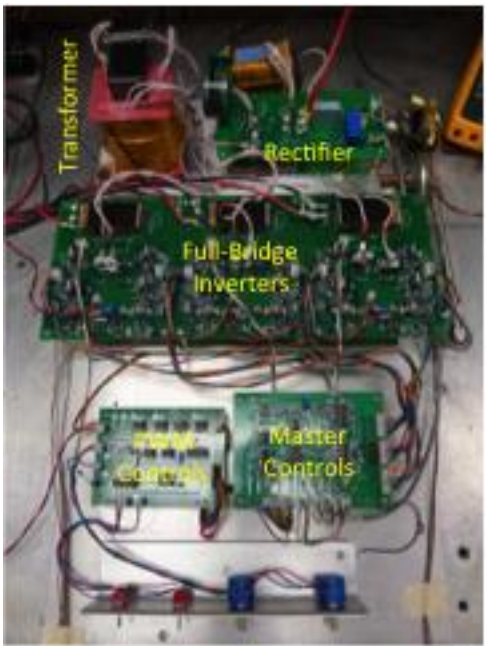

Fig. 29: Breadboard discharge module.

the derating requirements for the power semiconductors. A full bridge topology was chosen because it has low voltage stress on the power transistors and good transformer utilization making it a good choice for high-power applications. A switching frequency of 20 kHz was used to maintain switching losses as low as possible and to maximize efficiency. At full power the module processes as much as 7.5 kW. A new circuit was developed for this design to provide gate drives with the high voltage and speed required by the SiC MOSFETs to operate with very low switching losses. Preliminary measurements revealed efficiencies around 97 %.

Future work will focus on refining and optimizing the module design so that it has full functionality of a flight unit. A vacuum compatible brassboard unit will be designed and built to start addressing the thermal and packaging issues while using a highly modular slice architecture.

IV. SUMMARY

NASA's Human Exploration Framework Team identified high-power electric propulsion (EP) as an enabling technology for NASA human exploration missions. NASA's Office of the Chief Technologist (OCT) Game Changing Division (GCD) is funding a solar EP technical demonstration mission and technology development projects that are developing and maturing and will eventually demonstrate high-power Hall thruster technologies in space.

Under NASA's OCT GCD In-Space Propulsion technology program, NASA Glenn has been engaged in developing and testing of high-power Hall thrusters. Performance evaluations of the NASA-300M (20 kW) and NASA-457Mv2 (50 kW) thrusters indicated that both thrusters achieved peak total thrust efficiencies above 65%. Detailed plasma measurements performed in the near-field of the NASA-300M and NASA-457Mv2 thrusters, provided great insights as to the location of the ionization and acceleration zones and indicated close correlation between the plume structure and the magnetic field topology. Internal discharge chamber and far-field mappings were also performed on the NASA-300M and analysis of acquired data is ongoing. The internal discharge chamber measurements will further help us evaluate and assess thruster lifetime and can be used to further anchor the NASA Jet Propulsion Laboratory (JPL) physics-based Hall thruster model. The far-field data will be used to assess thruster efficiency loss mechanisms and thruster/spacecraft interactions. Thermal modeling of the NASA-300M and NASA-457Mv2 thrusters was also performed and compared well with measured temperatures. Detailed structural modeling of the NASA-457Mv2 was also performed. Model results will be compared to upcoming measurements from a random vibration test of the NASA-457Mv2. All the above mentioned tests and modeling efforts have greatly improved our understanding of high-power Hall thruster physics and will be leveraged in the design of high-efficiency long-life Hall thrusters for NASA missions.

In addition to testing and developing high-power Hall thrusters, the NASA Glenn is also developing a high-current hollow cathode for integration with high-power Hall thrusters. A hollow cathode assembly was operated at 100 A and at emitter temperatures that are consistent with long life. Finally, the NASA Glenn is also developing high-power, high-performance discharge modules for power processing units that will be used to power the high-power Hall thrusters.

ACKNOWLEDGMENTS

The authors would like to thank and acknowledge the Office of the Chief Technologist (OCT) Game Changing Division for funding this work. Contributions in this paper came from various members of the OCT In-Space Propulsion (ISP) team at NASA Glenn including Li Chang, Lauren Clayman, Thomas Haag, Daniel Herman, Wensheng Huang, Luis Pinero, Rohit Shastry, George Soulas, Jonathan Van Noord, and John Yim. The authors would also like to thank that many technicians that supported the execution and completion of the many tasks highlighted in this paper including Kevin Blake, Mark Forrester, Larry Hambley, George Jacynycz, Terrell Jansen, John Lauerhahs, Kevin McCormick, Michael Pastel, Derrick Patterson, and George Readus.

References

[1] Dudzinski, L., et al., "Design of Solar Electric Propulsion Transfer Vehicle for a Non-Nuclear Human Mars Exploration Architecture," IEPC Paper 99-181, October 1999.

[2] Oleson, S.R., et al., "Advanced Propulsion for Space Solar Power Satellites," AIAA Paper 99-2872, June 1999.

[3] Oleson, S.R., et al., "Mission Advantages of Constant Power Variable Specific Impulse Electrostatic Thrusters," NASA TM-2000-210477, March 2000.

[4] http://www.nasa.gov/exploration/new_space_enterprise/home/heft_summary.html

[5] Brophy, J.R., et al., "300-kW Solar Electric Propulsion System Configuration for Human Exploration of Near Earth Asteroids," AIAA Paper 2011-5514, August 2011.

[6] Smith, B., Nazario, M. L., and Manzella, D. H., "Advancement of a 30kW Solar Electric Propulsion System Capability for NASA Human and Robotic Exploration Mission," IAC-12-C4.4.2.

[7] Jankovsky, R.S., et al., "Preliminary Evaluation of a 10 KW Hall Thruster," AIAA Paper 99-0456, January 1999.

[8] Mason, L.S., et al., "1000 Hours Testing of a 10 KW Hall Effect Thruster," AIAA Paper 2001-3773, July 2001.

[9] Jankovsky, R.S., et al., "NASA's Hall Thruster Program 2002," AIAA Paper 2002-3675, July 2002.

[10] Manzella, D. H., et al., "Laboratory Model 50 kW Hall Thruster," AIAA Paper 2002-3676, July 2002.

[11] Jacobson", D. T., et al., "NASA's 2004 Hall Thruster Program," AIAA Paper 2004-3600, July 2004.

[12] Peterson, P. Y., "Performance and Wear Characterization of a High Power High–Isp Hall Thruster," AIAA Paper 2005-4243, July 2005.

[13] Kamhawi, H., Haag, T. W., Jacobson, D. T., and Manzella, D. H., "Performance Evaluation of the NASA-300M 20 kW Hall Effect Thruster," AIAA Paper 2011-5521, July 2011.

[14] Hofer, R. R., Peterson, P. Y., and Gallimore, A. D., "A High Specific Impulse Two-Stage Hall Thruster with Plasma Lens Focusing," IEPC Paper 01-036, October 2001.

[15] Hofer, R. R., and Gallimore, A. D., "The Role of Magnetic Field Topography in Improving the Performance of High-Voltage Hall Thrusters," AIAA Paper 2002-4111, July 2002.

[16] Manzella, D.M., "Scaling Hall Thrusters to High Power," Ph.D. Dissertation, Department of Mechanical Engineering, Stanford University, Stanford, CA, June 2005.

[17] Mercer, C.R., et al., "Benefits of Power and Propulsion Technology for a Piloted Electric Vehicle to an Asteroid," AIAA Paper 2011-7252, September 2011.

[18] Soulas, G. C., Haag, T. W., Herman, D. A., Huang, W., Kamhawi, H. et al., "Performance Test Results of the NASA-457M v2 Hall Thruster," AIAA Paper 2012-3940, July 2012.

[19] Mikellides, I. G., Katz, I., Kamhawi, H., and Vannoord, J. L., "Numerical Simulations of a 20-kW Class Hall Thruster Using the Magnetic-Field-Aligned-Mesh Code Hall2De," IEPC Paper 2011-244, September 2011.

[20] Jameson, K. K., Goebel, D. M., Hofer, R. R., and Watkins, R. M., "Cathode Couplings in Hall Thrusters," IEPC Paper 2007-278, September 2007.

[21] Huang, W., Shastry, R., Herman, D. A., Soulas, G. C., and Kamhawi, H., "Ion Current Density Study of the NASA-300M and NASA-457M v2 Hall Thrusters," AIAA Paper 2012-3870, July, 2012.

[22] Herman, D. A., Shastry, R., Huang, W., Soulas, G. C., and Kamhawi, H., "Plasma Potential and Langmuir Probe Measurements in the Near-field Plume of the NASA 300M Hall Thruster," AIAA Paper 2012-4115, July 2012.

[23] Shastry, R., Huang, W., Herman, D. A., Soulas, G. C., and Kamhawi, H., "Plasma Potential and Langmuir Probe Measurements in the Near-field Plume of the NASA 457Mv2 Hall Thruster," AIAA Paper 2012-4196, July 2012.

[24] Reid, B. M., "The Influence of Neutral Flow Rate in the Operation of Hall Thrusters," Ph.D. Dissertation, Aerospace Engineering, University of Michigan, Ann Arbor, MI, 2008.

[25] Brown, D. L., "Investigation of Flow Discharge Voltage Hall Thruster Characteristics and Evaluation of Loss Mechanisms," Ph.D. Dissertation, Aerospace Engineering, University of Michigan, Ann Arbor, MI, 2009.

[26] Kim, V., "Main physical features and processes determining the performance of stationary plasma thrusters," *Journal of Propulsion and Power*, Vol. 14, No. 5, 1998, pp. 736-743.

[27] Hofer, R. R., "Development and Characterization of High-Efficiency, High-Specific Impulse Xenon Hall Thrusters," Ph.D. Dissertation, Aerospace Engineering, University of Michigan, Ann Arbor, MI, 2004.

[28] Huang, W., Kamhawi, H., and Shastry, R., "Farfield Ion Current Density Measurements before and after the NASA HiVHAc EDU2 Vibration Test," AIAA Paper 2012-4195, July 2012.

[29] Hershkowitz, N., in *Plasma Diagnostics: Discharge Parameters and Chemistry*, edited by Flamm, D. L. (Academic Press, Inc., 1989), pp. 113-181.

[30] Lieberman, M. A. and Lichtenberg, A. J., *Principles of Plasma Discharges and Materials Processing*, Second ed. (John Wiley & Sons, Inc., Hoboken, NJ, 2005).

[31] Williams, G. J., Soulas, G. C., and Kamhawi, H., "Advanced Diagnostic Characterization of High-Power Hall Thruster Wear and Operation," AIAA Paper 2012-4036, July 2012.

[32] Mikellides, I.G., et al., "Magnetic Shielding of the Channel Walls in a Hall Plasma Accelerator," Phys. Plasmas, 18, 3, 033501 1-18 (2011).

[33] Mikellides, I.G., *et al.*, "Design of a Laboratory Hall Thruster with Magnetically Shielded Channel Walls, Phase I: Numerical Simulations," AIAA Paper 2011-5809.

[34] Kamhawi, H., and Van Noord, J., "Development and Testing of High Current Hollow Cathodes for High Power Hall Thrusters," AIAA Paper 2012-4080, July 2012.

[35] Carpenter, C. B., and Patterson, M. J., "High-Current Hollow Cathode Development," IEPC Paper 01-274, October, 2001.
[36] John, J. W., Sarver-Verhey, T. R., and Kamhawi, H., "High Current Cathode Development for 50 kW Class Hall Thruster," AIAA Paper 2005-4244, July 2005.